# Microstructure and Tribological Properties of WC Reinforced Iron-based Hardfacing Alloy

IOP Conf. Series: Materials Science and Engineering **493** (2019) 012093 doi:10.1088/1757-899X/493/1/012093

# Microstructure and Tribological Properties of WC Reinforced Iron-based Hardfacing Alloy

**Xin Jin [1, 2, *], Yi Li [1, 2], Bo Chen [1, 2], Huiji Fan [1, 2], Kun Feng [1, 2], Haixia Cui [1, 2]**

[1] Jiangsu XCMG Construction Machinery Research Institute Ltd., Xuzhou, China
[2] State Key Laboratory of Intelligent Manufacturing of Advanced Construction Machinery, Xuzhou Construction Machinery Group, Xuzhou, China

*Corresponding author e-mail: torresjin@126.com

**Abstract**. In this paper, WC reinforced and non-reinforced iron-based hardfacing alloys were deposited by PTA welding. Influence of WC particles on the hardfacing alloy was revealed by analysing the microstructure, microhardness and wear behavior. The results show that the matrix metals of the two hardfacing alloys are similar in structure. The primary carbides $(Fe, Cr)_7C_3$ and eutectic carbides are distributed on the cryptocrystalline martensite and residual austenite. The distribution of the large WC particles in the whole hardfacing alloy are relatively uniform, compared with the non-reinforced hardfcing alloy, the WC reinforced hardfacing alloy exhibits higher microhardness and better wear resistance property.

## 1. Introduction

Tungsten carbide (WC) is a widely used cemented carbide material, which has low reactivity and good wettability with iron-based alloys [1]. Therefore, WC particles are often added to iron-based alloys to prepare high-performance hardfacing alloy. Most researches on this field have been carried out using "conventional" reinforcement particle size (i.e. between 30 and 300μm), but the effect that larger particles (i.e. millimeter sized-WC) could have on the properties has rarely been discussed [2]. The millimeter-sized WC is mostly made of broken cemented carbide, which is low in cost and easy to recycle. In this paper, a large particle WC reinforced iron-based alloy was prepared by plasma transferred arc welding. The microstructure and microhardness of the two alloys with and without WC particles were compared, and the effect of WC particles on wear behavior was studied.

## 2. Material and Experimental Procedures

The Q235 steel plate with dimension of 60×150×30mm was used as substrate. The reinforcement particles adopted were sintered WC containing 5%Co with the size of 1.5 to 2.5 mm. The content of WC added (mass fraction) was 20%. The surfacing powder was Fe60 iron-based alloy powder, and the chemical composition was shown in Table 1.

The WC particle reinforced hardfacing alloy was prepared by synchronous two-way powder feeding method. The plasma transferred arc (PTA) welding process was performed using PTA-400E plasma arc surfacing apparatus. The deposition conditions for PTA welding used in this study were listed in Table 2.

After deposition, the cross section of alloys were ground flat to obtain smooth surfaces and polished with diamond paste for microscopic inspection and subsequent mechanical properties characterization. The microstructure and worn morphologies were examined by optical microscope and scanning electron microscopy (SEM) equipped with energy-dispersive spectrometer (EDS).The Vickers microhardness was measured by microhardness tester with a load of 0.98N for 15s.

The abrasion test was assessed by pin-on-disk tests in dry conditions. The loading force, the speed and loading time was 300N, 180r/min, and 3600s respectively. The alloys were cut into a pin-shaped sample of 25×10×10 mm, and a SiC grinding disk was selected as the friction pair. The wear resistance of alloys was characterized by wear mass loss.

**Table 1.** Chemical composition of Fe60 (wt/%)

| C | Cr | Ni | Si | Mo | Fe |
|---|---|---|---|---|---|
| 3.0 | 38 | 1.8 | 1.5 | 1.0 | Bal. |

**Table 2.** PTA process parameters

| Item | Non-reinforcement hardfacing alloy | WC reinforcement hardfacing alloy |
|---|---|---|
| Arc current/A | 145 | 145 |
| Arc voltage/V | 22 | 22 |
| Shield gas flow(Ar)/(L·h$^{-1}$) | 800 | 800 |
| Plasa gas flow(Ar)/(L·/h$^{-1}$) | 300 | 300 |
| Travel speed/(mm·s$^{-1}$) | 5 | 5 |
| Fe60 powder feed rate/(g·min$^{-1}$) | 40 | 40 |
| WC particle feed rate/(g·min$^{-1}$) | / | 5 |

## 3. Results and discussion

### *3.1. Microstructures*

The microstructure of two alloys near the fusion line is shown in figure 1. As can be seen from figures 1a and 1b, the matrix metals of the two hardfacing alloys are similar in structure. The primary carbides and eutectic carbides are distributed on the cryptocrystalline martensite and residual austenite. The primary carbides are cylindrical in shape, hexagonal in cross section and small voids in the interior. This is a typical $M_7C_3$ carbide, and the growth of primary carbides is obviously directional [3]. Figures 1c and 1d exhibit that the addition of large WC particles has an effect on the growth direction of the primary carbide, but does not significantly change the microstructure of the matrix metals.

Figure 2a exhibits that the large WC particles are relatively uniformly distributed in the whole alloy, which is significantly different from the phenomenon that micron-sized WC particles are easily precipitated at the bottom of the alloy. Since the density of WC particles is greater than that of the matrix metal and the temperature of molten pool is high, the WC particles have a long residence time at a high temperature and a slow cooling rate, so that the WC particles are prone to sink during cooling and solidification [4]. However, due to the large size of WC particles and the mutual obstruction during the sinking process, WC particles stack upward and exist in the upper, middle and lower parts of hardfacing alloy. As shown in Figure 2b, the large WC particle is dissolved slightly, and only a small amount of W element is diffused. The edges of the WC particles are well bonded to the metal matrix without significant holes and cracks. The energy spectrum analysis is performed on the region of A, B, C and D in Figure 2c and Figure 2d, and the results are shown in Table 3. Phase A is the original WC, and Phase B is the newly precipitated WC after dissolution. The phase C is a primary carbide $(Fe,Cr)_7C_3$ of Fe and Cr. Phase D is a fishbone-like eutectic structure, which is a new structure formed by the diffusion of

W element of WC particles into matrix metals, resulting in the increase of W element content in eutectic carbides [5].

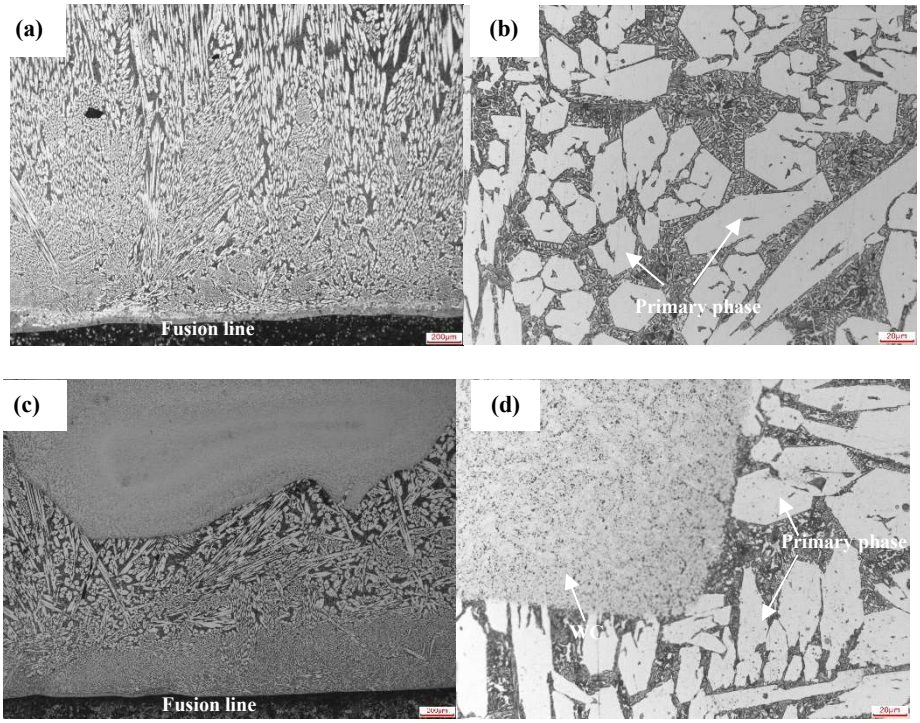


**Figure 1.** Microstructure of non-reinforced and WC reinforced hardfacing alloys (a) Non-reinforced hardfacing alloy (50×); (b) Non-reinforced hardfacing alloy (500×); (c) WC reinforced hardfacing alloy (50×); (d)WC reinforced hardfacing alloy (500×)

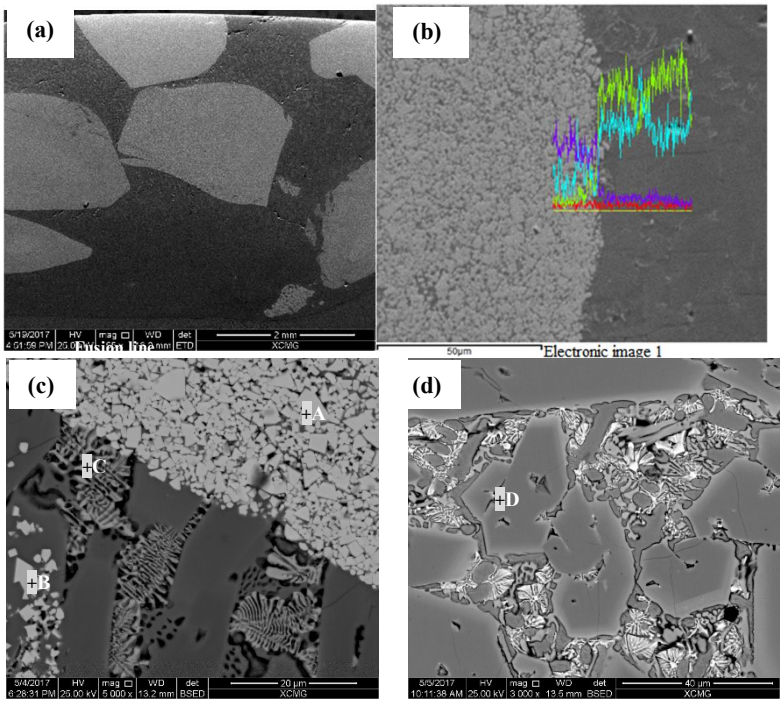


**Figure 2.** SEM morphologies of WC reinforced hardfacing alloy

**Table 3.** The EDS analysis results of hardfacing alloys (at/%)

| | C | Cr | Co | W | Fe |
|---|---|---|---|---|---|
| A | 59.10 | 2.15 | 0.12 | 37.63 | 1.00 |
| B | 65.90 | 3.18 | 0.20 | 29.10 | 1.62 |
| C | 38.45 | 11.26 | / | 20.47 | 29.82 |
| D | 34.27 | 39.78 | / | / | 25.95 |

### *3.2. Microhardness*

Figure 3 indicates the microhardness profiles along the depth of cross section of the WC reinforced hardfacing alloy and non-reinforced hardfacing alloy. It can be observed that the Q235 steel substrate has an average microhardnss of approximately HV 190. Due to the presence of high hardness carbides and solid solution strengthening of Si and Cr elements in the alloy, the non-reinforced hardfacing alloy has average microhardness of approximately HV 880. Meanwhile, compared with the non-reinforced hardfacing alloy, the microhardness of WC reinforced hardfacing alloy is furtherly increased due to the solid solution strengthening of the W element and the dispersion strengthening of the WC particle [6]. The peak at the curve is the hardness of the WC particles.

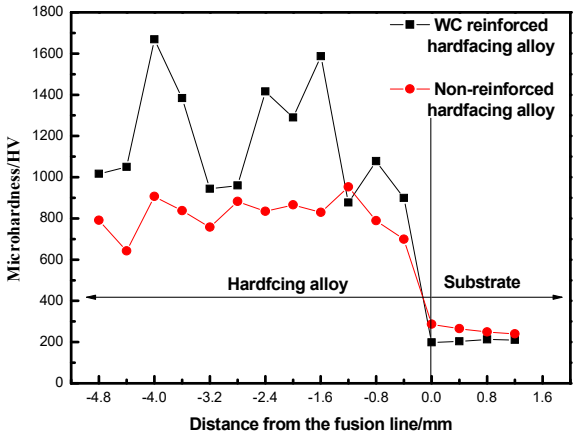


**Figure 3.** Microhardness distribution of cross section of the WC reinforced and non-reinforced hardfacing alloys

### *3.3. Wear behavior*

Figure 4 shows the histogram of wear capacity of two alloys. It can be observed that the wear mass loss of non-reinforced hardfacing alloy is about twice as much as that of WC reinforced hardfacing alloy. The wear resistance of WC reinforced hardfacing alloy has obvious advantage.

Figure 5 shows the worn morphology of the two alloys. As can be seen from figure 5a and 5b, the wear mechanism of the two alloys is mainly plastic deformation (including plough groove and micro-cutting). The wear marks of the WC reinforced hardfacing alloy are shallow and thin, but the wear marks of the non-reinforced hardfacing alloy are deep and wide. The worn large WC particles are relatively intact without obvious flaws. This is due to the cohesion of Co and the interaction of fine particles in the large WC particles, which makes the sintered WC particles have better resistance to abrasive impact [7], therefore, the large WC particles do not crack during wear process. In the early stage of wear, WC particles are on the same plane with metal matrix and substrate. Because of the relatively low hardness of the metal matrix, micro-cutting and ploughing grooves are generated. As the wear process progresses, metal matrix is first recessed compared to the WC particles. The WC particles are exposed, at which point the load acts directly on the WC particles [8]. The integrity of the WC particles significantly enhances the abrasion resistance of the alloy, therefore, the wear resistance of the large WC particle reinforced hardfacing alloy is better than that of the non-reinforced hardfacing alloy.

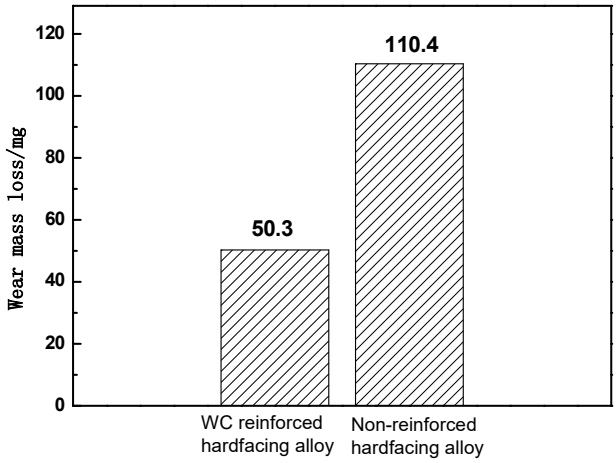


**Figure 4.** Histogram of wear capacity

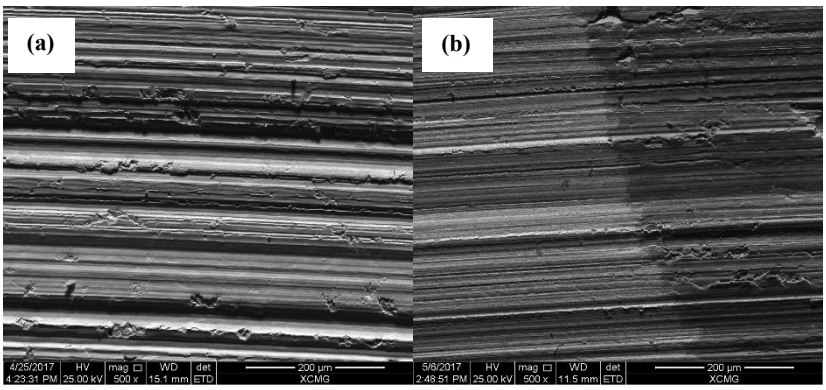


**Figure 5.** Worn morphologies of non-reinforced (a) and WC reinforced (b) hardfacing alloys

## 4. Conclusion

In this paper, the microstructure and tribological properties of WC reinforced iron-based hardfacing alloy on Q235 steel were investigated. The following conclusions can be drawn.

1) The matrix metals of the two hardfacing alloys are similar in structure. The primary carbides and eutectic carbides are distributed on the cryptocrystalline martensite and residual austenite.

2) The large WC particles are relatively uniformly distributed in the whole alloy.

3) The hardness of WC reinforced hardfacing alloy is higher than that of non-reinforced hardfacing alloy.

4) The wear resistance of the WC reinforced hardfacing alloy is better and the large WC particles remain relatively intact during the wear process.

## References

[1] Tang X H, Chung R, Pang C J, et al. Microstructure of high (45%) chromium cast irons and their resistances to wear and corrosion [J]. Wear, 2011, 271(9): 1426-1431.

[2] D. Dechuyteneer, F. Petit, M. Gonon, et al. Influence of large particle size-up to 1.2mm-and morphology on wear resisitance in NiCrNSi/WC laser cladded composite coatings [J]. Surface& Coating Technology, 311(2017), 365-373.

[3] Wang Q B, Wang Z H, Li S M. Microstructure and properties of the Fe-Cr-C hardfacing alloys with high carbon content [J]. Transactions of the China Welding Institution, 2004, 25(6):119-123.

[4] Qu S Y, Wang X H, Zou Z D, et al. The heat damage mechanism of WC Cemented carbide for

hardfacing [J]. Transactions of the China Welding Institution, 2001, 22(2):85-88.
[5] Zhang G D, Li L, Cao H M. Structure and properties of WC reinforced high cast iron surfacing layer desposited by plasma arc welding [J]. China Surface Engineering, 2015, 28(6):111-118.
[6] Wang W, Qian S Q , Zhou X Y. Microstructure and properties of TiN/Ni composite coating prepared by plasma transferred arc scanning process [J]. Transactions of Nonferrous Metals Society of China, 19(2009), 1180-1184.
[7] Wang Z H, He D Y. Microstructure and properties of the Fe-Cr-C hardfacing alloy strengthened by NbC [J]. Transactions of the China Welding Institution, 2007, 28(2):55-58.
[8] Li Z L, Jiang Y H, Zhou R. Study on three-body abrasive wear performance of cast iron matrix surface composites wc parties reinforced [J] . China Mechanical Engineering, 2006, 18(17), 1967-1971.